

Effect of Feedback Coil and Plasma Rotation on Nonlinear Resistive Wall Mode in a Cylindrical Tokamak

SATO Masahiko and NAKAJIMA Noriyoshi

National Institute for Fusion Science, Toki 509-5292, Japan

(Received: 10 December 2003 / Accepted: 10 May 2004)

Abstract

Nonlinear behavior of resistive wall mode (RWM) is investigated using reduced MHD equations. For fixed plasma rotation velocity, The linear growth rate of RWM with poloidal rotation increases as the resistive wall become close to the plasma surface. Thus, the poloidal rotation velocity required to stabilize the linear RWM increases. However, when the poloidal rotation frequency is sufficiently large, the nonlinear saturation amplitudes are small. Also feedback stabilization of the RWM without the poloidal rotation has been studied. The linear growth rate decreases due to the external magnetic field produced by the feedback coil. However, low saturation level can not be obtained.

Keywords:

resistive wall mode, plasma rotation, nonlinear saturation, tokamak

1. Introduction

Magnetohydrodynamic (MHD) stability of magnetically confined plasmas is crucial for obtaining improved confinement suitable for a fusion reactor [1]. For obtaining high beta plasmas, stabilization of dangerous ideal kink modes is required in current carrying tokamaks [2]. The ideal kink modes can be stabilized by a perfect conducting wall placed sufficiently close to the plasma surface [3]. However, when the wall has a finite conductivity, the mode can not be stabilized completely, even if the wall is close to the plasma surface [4]. In this situation, resistive wall modes (RWMS) become unstable. The RWM grows slowly with a growth time on the order of resistive decay time of magnetic field, τ_w , in a wall. For a stationary tokamak sustained with a large bootstrap current, such a slowly growing instability becomes dangerous and it is important to stabilize RWMS. There are several experimental results that the RWMS deteriorate confinement in tokamaks [5-7]. For suppressing effects due to RWMS feedback controls have been proposed [8,9].

It is noted that the linear RWMS can be stabilized by plasma rotation [10-14]. From nonlinear simulations, M. Sato *et al.* [15] showed that the magnetic perturbation due to the RWM has a role to suppress the poloidal rotation through the Maxwell stress and the resultant slowdown of plasma rotation significantly affects stability of RWMS and their nonlinear behavior. In this paper we studied nonlinear RWMS for the case that resistive wall is close to the plasma surface. For such a case, the destabilizing effect for linear RWMS due to plasma rotation appears [4,14].

The rest of the paper is organized as follows. In Sec. 2, the reduced MHD equations for low beta cylindrical plasmas

are introduced. Then our numerical model for studying nonlinear RWMS are shown. Numerical schemes for solving the reduced MHD equations are briefly mentioned. In Sec. 3, results of nonlinear calculations of unstable RWMS are shown. Finally, a summary is given in Sec. 4.

2. Numerical model

For low beta cylindrical tokamak plasmas, the well-known reduced MHD equations were derived by Kadomtsev and Pogutse, and Strauss [16,17]. These equations with dimensionless variables are shown as

$$\frac{\partial \psi}{\partial t} = \frac{\partial \phi}{\partial r} \frac{1}{r} \frac{\partial \psi}{\partial \theta} - \frac{1}{r} \frac{\partial \phi}{\partial \theta} \frac{\partial \psi}{\partial r} - \frac{\partial \phi}{\partial \zeta} + \eta J_\zeta - E_\zeta, \quad (1)$$

$$\begin{aligned} \frac{\partial U}{\partial t} = & \frac{\partial \phi}{\partial r} \frac{1}{r} \frac{\partial U}{\partial \theta} - \frac{1}{r} \frac{\partial \phi}{\partial \theta} \frac{\partial U}{\partial r} + \frac{\partial J_\zeta}{\partial r} \frac{1}{r} \frac{\partial \psi}{\partial \theta} - \frac{1}{r} \frac{\partial J_\zeta}{\partial \theta} \frac{\partial \psi}{\partial r} \\ & - \frac{\partial J_\zeta}{\partial \zeta} + \nu \nabla_\perp^2 U + S_m, \end{aligned} \quad (2)$$

$$J_\zeta = \nabla_\perp^2 \psi, \quad (3)$$

$$U = \nabla_\perp^2 \phi, \quad (4)$$

in the cylindrical coordinates (r, θ, ζ) , where ψ is the poloidal magnetic flux defined by $\mathbf{B}_\perp = -\frac{a}{R} \nabla \psi \times \mathbf{e}_\zeta$ and ϕ is the stream function defined by $\mathbf{v}_\perp = \nabla \phi \times \mathbf{e}_\zeta$, and \perp means perpendicular to the toroidal direction. Here, r , θ and ζ are radial, poloidal and toroidal coordinate, respectively. In eq. (1), resistivity η is normalized to $\mu_0 a^2 / \tau_{hp}$, where $\tau_{hp} = R \sqrt{\mu_0 \rho} / B_0$. Here the length of cylindrical plasma is $2\pi R$, the plasma

Corresponding author's e-mail: masahiko@nifs.ac.jp

minor radius is a , the mass density is ρ , and the longitudinal magnetic field is B_0 . In eq. (1), the electric field, E_ζ , is chosen to satisfy $\eta_{eq} J_{eq} = E_\zeta$, where η_{eq} and J_{eq} are a resistivity and a current density at an equilibrium state, respectively. In eq. (2), viscosity is denoted by v . The source term S_m is chosen to satisfy $v \nabla_\perp^2 U_{eq}(r) + S_m = 0$, where $U_{eq}(r)$ is a vorticity at an equilibrium state. It is noted that a poloidal rotation is introduced through the vorticity $U_{eq}(r)$. In eqs. (1) and (2), time is normalized to τ_{hp} , length to a , ψ to $B_0 a^2$, ψ to $B_0 a^2 / \tau_{hp}$ and U to B_0 / τ_{hp} . Thus the velocity v_\perp is normalized with a / τ_{hp} .

Resistivity is introduced artificially in the vacuum region to use the pseudo-vacuum model [18,19]. For obtaining time evolution of resistivity in eq.(1), the equation of time evolution of electron temperature T_e is solved:

$$\frac{\partial T_e}{\partial t} = \frac{\partial \phi}{\partial r} \frac{1}{r} \frac{\partial T_e}{\partial \theta} - \frac{1}{r} \frac{\partial \phi}{\partial \theta} \frac{\partial T_e}{\partial r} + \chi_\perp \nabla_\perp^2 T_e + Q, \quad (5)$$

where the perpendicular thermal transport coefficient of electron temperature is normalized to χ_\perp to a^2 / τ_{hp} . The resistivity is assumed to be proportional to $T_e^{-3/2}$. In the numerical calculations $\chi_\perp = 10^{-8}$ are assumed. The source term Q is chosen to satisfy $\chi_\perp \nabla_\perp^2 T_{eq}(r) + Q = 0$, where $T_{eq}(r)$ is a temperature at an equilibrium state.

The main plasma is located in the region $r \leq 1$, the resistive wall in the region $r_w \leq r \leq r_w + d_w$, and the pseudo-vacuum in the region $1 < r < r_w = 1.1$ and $r_w + d_w < r < r_c$. It is assumed that a perfect conducting wall is located at $r_c = 2$.

In the region $r > r_w$, the velocity is zero and the resistivity is independent of time. However, the poloidal flux may change in this region. Thus, the diffusion equation of perturbed poloidal flux $\tilde{\psi}$

$$\frac{\partial \tilde{\psi}}{\partial t} = \eta \nabla_\perp^2 \tilde{\psi} \quad (6)$$

is solved.

The boundary conditions for the reduced MHD equations solving $\tilde{\phi}(r, \theta, \zeta, t)$, $\tilde{\psi}(r, \theta, \zeta, t)$ and $\tilde{T}_e(r, \theta, \zeta, t)$ are $\tilde{\phi}(r_w) = \tilde{T}_e(r_w) = 0$ at $r = r_w$ and $\tilde{\psi}(r_c) = 0$ at $r = r_c$. At $r = 0$ standard boundary conditions are employed.

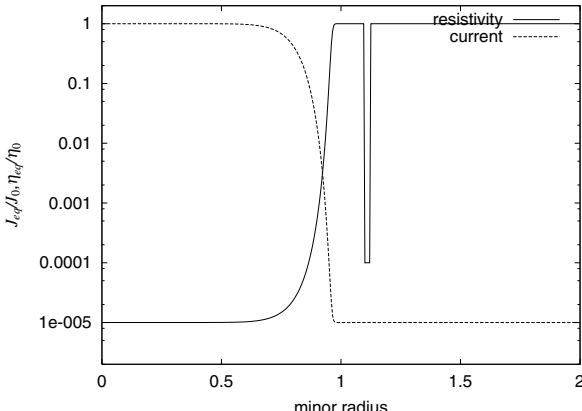


Fig. 1 Profile of plasma current density J_{eq} and resistivity η_{eq} at equilibrium state.

The current profile at an equilibrium state is chosen as

$$J_{eq}(r) = (J_a - J_b)(1 - r^{12})^{12} + J_b \quad (7)$$

for $0 \leq r \leq 1$, and $J_{eq}(r) = J_b \ll J_a$ for $1 < r < r_c$. The resistivity profile is assumed to be proportional to $1/J_{eq}(r)$ for $r < r_w$. $\eta(r=0)$ and the resistivity in the pseudo-vacuum region η_v are set to be $\eta(r=0) = 10^{-5}$ and $\eta_v = 1$, respectively. Resistivity of the resistive wall η_w is assumed to be $\eta_w = 10^{-4}$. The profiles of J_{eq} and η_{eq} are shown in Fig. 1. The rational surface of $q = 2$ is located at $r = r_s \approx 1.08$ in the pseudo-vacuum region. When a perfect conducting wall is located at $r = 1.45$, the ideal external kink modes are stabilized perfectly.

Equations (1)–(5) are solved numerically for the cylindrical plasma shown in Fig. 1. In our numerical code, the radial derivates are replaced with standard difference approximations. The derivatives with respect to poloidal angle θ and the toroidal angle ζ are treated with Fourier-expansions. We also assume single helicity for studying the $(m,n) = (2,1)$ mode destabilized at the $q = 2$ surface. The time advancement is made with a predictor-corrector method.

3. Numerical results

Figure 2 shows dependence of linear growth rate of $(m,n) = (2,1)$ mode on the rigid poloidal rotation frequency $\omega = v_\theta / r$ and the resistive wall position r_w . Here v_θ is a poloidal flow velocity proportional to r . For $\omega \sim 0.2$, the mode is stabilized as the resistive wall is moved farther from the plasma, which is consistent with the theoretical prediction. When poloidal rotation is sufficiently large, the RWM is perfectly stabilized.

Figure 3 shows time evolution of magnetic energy, E_M , of $(m,n) = (2,1)$ component for $r_w = 1.1$ for various poloidal rotation frequencies. Because of limitation of our numerical code, we carried out simulations for $E_M \leq 0.01$. When the resistive wall is close to the plasma surface, the poloidal rotation velocity required to stabilize the RWM becomes larger. However, when the initial poloidal rotation velocity is large, the amplitudes of the perturbed magnetic energy saturate at a low level while the large poloidal rotation

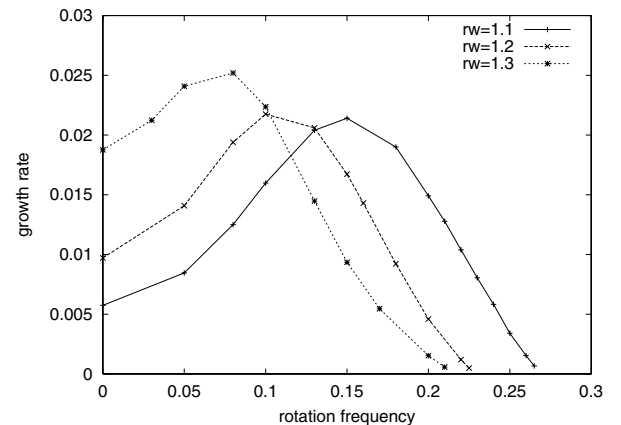


Fig. 2 Dependence of linear growth rate of $(m,n) = (2,1)$ mode on rigid poloidal rotation frequency.

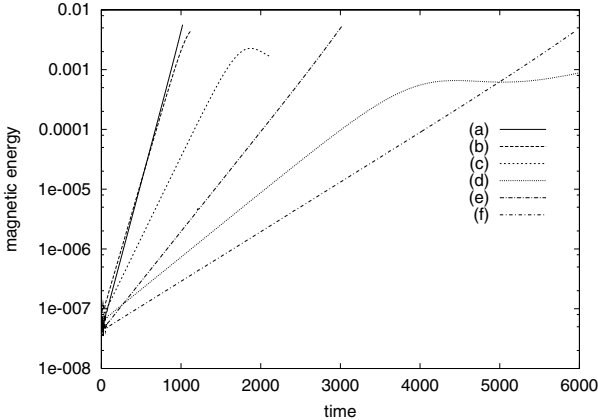


Fig. 3 Time evolution of magnetic energy of $(m,n) = (2,1)$ component for various poloidal rotation frequencies. (a) $\omega = 0$, (b) $\omega = 0.24$, (c) $\omega = 0.25$ and (d) $\omega = 0.26$. (e) and (f) are results with feedback coil. (e) $\alpha = 40$ and (f) $\alpha = 50$.

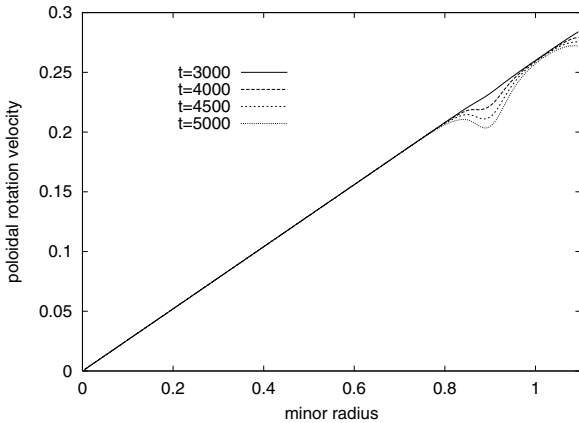


Fig. 4 Time evolution of radial profile of poloidal rotation velocity for $r_w = 1.1$ and $\omega = 0.26$.

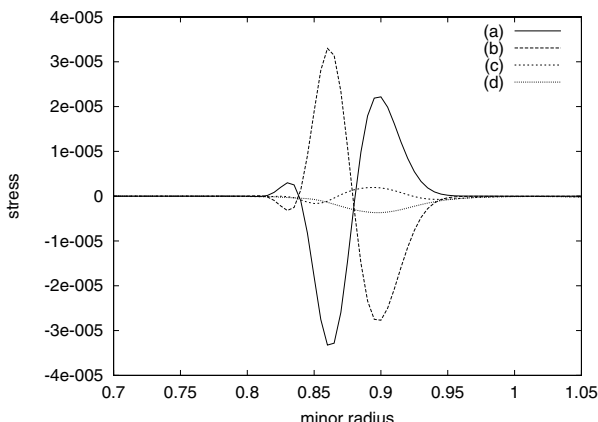


Fig. 5 Radial profile of each term in eq. (9) for $r_w = 1.1$ and $\omega = 0.26$ at $t = 3000$. Here curve (a) denotes the first term of right-hand side of eq. (9) corresponding to Reynolds stress, curve (b) denotes the second term of RHS of eq. (9) corresponding to Maxwell stress, curve (c) denotes the third term of RHS of eq. (9) corresponding to viscous damping, and curve (d) denotes left-hand side of eq. (9).

remains such as the case for $\omega = 0.26$.

Figure 4 shows time evolution of profile of poloidal velocity for $r_w = 1.1$ and $\omega = 0.26$. There is a slowdown of poloidal rotation velocity at the plasma surface. The poloidal rotation velocity does not become zero at the plasma surface in the nonlinear regime. Thus, there is not nonlinear destabilization, which is seen in [15], due to the reduction of the poloidal rotation for $t \lesssim 5000$.

The time evolution of averaged poloidal rotation velocity $\langle v_\theta \rangle$ is described by

$$\frac{\partial \langle v_\theta \rangle}{\partial t} = -\frac{1}{r^2} \frac{\partial}{\partial r} r^2 \langle \tilde{v}_r \tilde{v}_\theta \rangle + \frac{1}{r^2} \frac{\partial}{\partial r} r^2 \langle \tilde{B}_r \tilde{B}_\theta \rangle - v \frac{d \tilde{U}_0}{dr}, \quad (8)$$

where $\langle f \rangle = \int_0^{2\pi} \int_0^{2\pi} f d\theta d\zeta / 4\pi^2$ and \tilde{U}_0 is $(m,n) = (0,0)$ component of perturbed vorticity. Figure 5 shows that radial profile of each term in eq. (9) for $r_w = 1.1$, $\omega = 0.26$ at $t = 3000$. As shown Fig. 5, the poloidal rotation decreases due to Maxwell stress similar to the case for $\eta_0/\eta_v = 10^2$ [15]. However, since the Reynolds stress is comparable to the Maxwell stress, a damping force is small, and then the reduction of poloidal rotation is small. Since the poloidal rotation continues to decrease as shown in Fig. 4, it seems that the RWM will grow again when the poloidal rotation becomes smaller than a critical level. If the poloidal rotation does not decrease by controlling the source term S_m in eq. (2), the saturated amplitudes of the RWM may keep at the low level.

Finally, effect of feed back coil on nonlinear RWM without rotation is studied. For modeling of feed back coil, E_f is added in eq. (6) for $(m,n) = (2,1)$ component:

$$\frac{\partial \psi_{2,1}}{\partial t} = \eta \nabla_\perp^2 \psi_{2,1} - E_f g(r), \quad (9)$$

where $\psi_{2,1}$ is $(m,n) = (2,1)$ component of ψ . Equation (9) is solved in the pseudo-vacuum region. Here, $g(r)$ is chosen as $g(r) = 1$ for $1.15 \leq r \leq 1.17$ and $g(r) = 0$ for other region. It is also assumed that $E_f = \alpha \psi_w$, where ψ_w is the amplitude of $(m,n) = (2,1)$ component of ψ at the resistive wall. Thus, outside of the resistive wall, there is the external helical current, which is proportional to the amplitude of poloidal flux. When α is large, the linear growth rate become small as shown in Fig. 3. However, low saturation level can not be obtained.

4. Summary

Nonlinear behavior of the RWM of $(m,n) = (2,1)$ mode has been investigated with the reduced MHD model. There is an initial increase in the linear growth rate of RWMS with the poloidal rotation. However, when the poloidal rotation frequency is sufficiently large, the linear growth rate becomes small and the nonlinear saturation amplitudes decrease. The external magnetic field produced by the feedback coil can reduce the linear growth rates of the RWMS. However, nonlinear saturated amplitudes with the feedback stabilization

are not small when the poloidal rotation dose not exist.

References

- [1] F. Troyon *et al.*, Plasma Phys. Control. Fusion **26**, 1A, 209 (1984).
- [2] J.P. Freidberg, *Ideal Magnetohydrodynamics* (Plenum, New York, 1987).
- [3] V.D. Shafranov, Sov. Phys. Tech. Phys. **15**, 175 (1970).
- [4] J.M. Finn, Phys. Plasmas **2**, 198 (1995).
- [5] T.S. Taylor *et al.*, Phys. Plasmas **2**, 2390 (1995).
- [6] M. Okabayashi *et al.*, Nucl. Fusion **36**, 1167 (1996).
- [7] A.M. Garofalo *et al.*, Phys. Plasmas **6**, 1893 (1999).
- [8] A.H. Boozer, Phys. Plasmas **5**, 3350 (1998).
- [9] M. Okabayashi *et al.*, Phys. Plasmas **8**, 2071 (2001).
- [10] A. Bondeson and D.J. Ward, Phys. Rev. Lett. **72**, 2709 (1994).
- [11] R. Betti and J.P. Freidberg, Phys. Rev. Lett. **74**, 2949 (1995).
- [12] R. Fitzpatrick and A.Y. Aydemir, Nucl. Fusion **36**, 11 (1996).
- [13] C.G. Gimblett *et al.*, Phys. Plasmas **3**, 3619 (1996).
- [14] A. Yoshioka, T. Tatsuno and M. Wakatani, J. Phys. Soc. Jpn **67**, 3794 (1998).
- [15] M. Sato, S. Hamaguchi and M. Wakatani, Phys. Plasmas **10**, 187 (2003).
- [16] B.B. Kadomtsev and O.P. Pogutse, Sov. Phys. JETP **38**, 283 (1974).
- [17] H.R. Strauss, Phys. Fluids **19**, 134 (1976).
- [18] G. Kurita *et al.*, Nucl. Fusion **26**, 449 (1986).
- [19] Yu. N. Dnestrovskii *et al.*, Sov. J. Plasma Phys. **11**, 616 (1985).